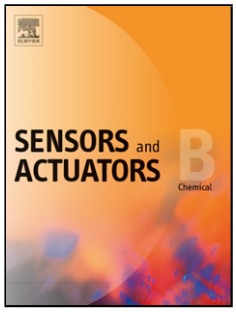

Title: Choline Oxidase Inhibition Biosensor Based on Poly(Brilliant Cresyl Blue) – Deep Eutectic Solvent / Carbon Nanotube Modified Electrode for Dichlorvos Organophosphorus Pesticide

Authors: Wanderson da Silva, Mariana Emilia Ghica, Christopher M.A. Brett

PII: S0925-4005(19)31061-5
DOI: https://doi.org/10.1016/j.snb.2019.126862
Article Number: 126862

Reference: SNB 126862

To appear in: *Sensors and Actuators B*

Received date: 9 May 2019
Revised date: 17 July 2019
Accepted date: 22 July 2019

Please cite this article as: da Silva W, Ghica ME, Brett CMA, Choline Oxidase Inhibition Biosensor Based on Poly(Brilliant Cresyl Blue) – Deep Eutectic Solvent / Carbon Nanotube Modified Electrode for Dichlorvos Organophosphorus Pesticide, *Sensors and amp; Actuators: B. Chemical* (2019), https://doi.org/10.1016/j.snb.2019.126862

Choline Oxidase Inhibition Biosensor Based on Poly(Brilliant Cresyl Blue) – Deep Eutectic Solvent / Carbon Nanotube Modified Electrode for Dichlorvos Organophosphorus Pesticide

Wanderson da Silva, Mariana Emilia Ghica, Christopher M.A. Brett*

Department of Chemistry, Faculty of Sciences and Technology, University of Coimbra, 3004-535 Coimbra, Portugal

*Corresponding author:

Tel: +351-239854470

Fax: +351-239827703

E-mail: cbrett@ci.uc.pt

Graphical abstract

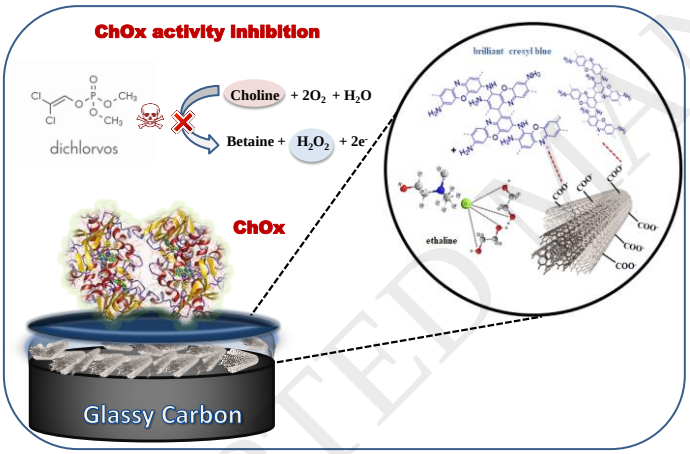

Highlights

- Poly(cresyl blue) (PBCB) films formed in ethaline DES and aqueous solution
- $PBCB_{DES}$ films formed by potentiostatic and potentiodynamic electropolymerisation
- $PBCB_{DES}$ films formed on carbon nanotubes have superior sensing properties to $PBCB_{aq}$
- Choline oxidase immobilized on $PBCB_{DES}$ films for enzymatic inhibition biosensor
- Nanomolar limit of detection for dichlorvos was achieved

Abstract

A novel electrochemical choline oxidase enzyme inhibition biosensor for dichlorvos has been developed based on poly(brilliant cresyl blue) films formed on multiwall-carbon nanotube modified glassy carbon electrodes by fixed potential and potentiodynamic cycling electropolymerisation in acid-doped ethaline deep eutectic solvent or aqueous medium. Film characterisation was done by voltammetry and scanning electron microscopy. The effect of the parameters used during potentiostatic polymerization, such as electrolyte solution (acid-ethaline or aqueous solution), polymerisation time and applied potential on the rate of growth and the electrochemical properties of the polymer films were studied. The choline oxidase enzyme inhibition biosensor for dichlorvos detection used the best polymer film formation conditions, in acid-doped ethaline. The type of reversible inhibition was determined. The new biosensor exhibited the lowest limit of detection for dichlorvos determination of those reported, 1.6 nM, excellent reproducibility and long-term stability, which makes it a promising tool for monitoring traces of organophosphorus pesticides in the environment.

Keywords: Deep eutectic solvent; brilliant cresyl blue electropolymerisation; carbon nanotubes; choline oxidase; electrochemical enzyme inhibition biosensor; dichlorvos

1 Introduction

Organophosphorus pesticides (OPS) play an important role in agricultural productivity due to their insecticidal activity. However, owing to their high acute toxicity and biocompatibility effects, their residues in the environment can provoke serious intoxication in living organisms [1–3]. In this regard, there have been big efforts and interest in applying new analytical methods with rapid response, that are low cost, accurate, reliable and sensitive for monitoring OPS residues in the environment as an alternative to classical analytical methods such as high-performance liquid chromatography [4], gas chromatography [5] and gas chromatography-mass spectrometry [6]. Although these methods are highly accurate, they are extremely expensive, require long time-consuming pre-treatment processes and highly specialized staff. In contrast,

enzyme-inhibition biosensors have offered the best choice for simple and rapid detection of toxic compounds due to minimum sample pre-treatment, more rapid analysis, high sensitivity and selectivity of some enzymes to toxic compounds used as inhibitors [7]. This type of biosensor is usually highly specific for a group of compounds, for example, pesticides or heavy metal ions due to the presence of binding sites in the structure of the enzymes, which bind these toxic compounds, in this way affecting their activity [8]. Furthermore, the nanomolar limit of detection that can be achieved is much lower than other electrochemical methods, less than the limits considered hazardous for living organisms, which make them promising for analytical purposes [9].

In recent decades, much progress has been made in applying nanomaterials such as metal nanoparticles, carbon materials and conducting polymers to design novel biosensors. They offer to biosensing platforms an increase of the surface transducing area, which in turn increases the sensitivity and often catalytic effects, besides preserving the enzymatic activity for a longer time period, due to their biocompatibility [10–12].

Deep eutectic solvents (DES) are formed by a binary mixture composed of a hydrogen bond donor (HBD) and an acceptor (HBA) mixed in a specific molar ratio. DES exhibit similar properties to traditional ionic liquids including high conductivity, stability, and a wide potential range (important properties in the electrochemical synthesis of polymers which often require a high overpotential for radical generation) compared with aqueous solutions. Other advantages are low cost, low toxicity and no requirement for time-consuming steps of synthesis, which make them ideal for biosensor applications [13,14].

This work describes for the first time the development of a highly sensitive enzyme inhibition biosensor for dichlorvos organophosphorus pesticide, with superior analytical properties to biosensors in the literature. It is based on choline oxidase (ChOx) immobilised on poly(brilliant cresyl blue) (PBCB) films electrodeposited in ethaline DES (choline chloride : ethylene glycol)

on multiwalled carbon nanotube (MWCNT) modified glassy carbon electrodes (GCE). PBCB films were formed by electropolymerisation in both potentiostatic and potentiodynamic mode in HNO_3 doped ethaline, the best acid dopant found in previous work [15].

The influence of the composition of the polymerization solution, applied potential and polymerisation time on the electropolymerization of BCB in potentiostatic mode were evaluated. PBCB films formed under the best experimental conditions were used as electrode substrate for ChOx immobilization. The analytical performance of the biosensor was evaluated: sensitivity, limit of detection, linear concentration range, and the degree of inhibition of ChOx as well as operational stability and reproducibility. The mechanism of inhibition was deduced by a new and simple graphical method [16] and was validated with the classical Dixon and Cornish-Bowden plots. Application was demonstrated using spiked orange juice.

2. Experimental

2.1 Reagents and solutions

Choline oxidase (from *Arthrobacter globiformis* activity 8-20 U mg^{-1}, CAS number: 9028-67-5), bovine serum albumin (BSA), glutaraldehyde (GA, 2.5% v/v in water), sulfuric acid (97 %), nitric acid (65 %), hydrochloric acid (37 %), acetic acid (94.74 %), choline chloride, and anhydrous ethylene glycol were purchased from Sigma-Aldrich, Germany. Brilliant cresyl blue dye (95 %) was purchased from Fluka, Switzerland. MWCNT with ~ 95 % purity, 30 ± 10 nm, and 1-5 length were from Nanolab, U.S.A. Dichlorvos PESTANAL®, analytical standard (from Sigma-Aldrich) was used for the study of enzyme inhibition. Phosphate buffer solutions (PB) with various pH values were prepared by mixing standard stock solutions of 0.2 M Na_2HPO_4 (Merck, Germany) and 0.2 M NaH_2PO_4 (Riedel De Haën, Germany) and adjusting the pH with 0.1 mM hydrochloric acid (37 %) or 0.1 mM sodium hydroxide (from Sigma-Aldrich).

All reagents were of analytical grade and were used without further purification. Millipore Milli-Q nanopure water (resistivity ≥ 18 MΩ cm) was used for the preparation of all solutions. Experiments were all performed at room temperature (25 ± 1 ºC).

2.2 Instrumentation

Voltammetric and amperometric experiments were carried out at room temperature with a computer controlled Ivium Compactstat potentiostat (Ivium Technologies B.V., Eindhoven, Netherlands). For all electrochemical experiments, a conventional three-electrode system consisting of a 0.00785 cm^2 geometric area glassy carbon electrode (GCE) as working electrode, a platinum wire counter electrode, and an Ag/AgCl (3M KCl) reference electrode were employed. A scanning electron microscope (SEM) (JEOL, JSM-5310, Japan) was used to characterize the PBCB films electrodeposited on MWCNT-modified carbon film electrodes. The pH measurements were done with a CRISON 2001 micro pH-meter (Crison Instruments SA, Barcelona, Spain).

2.3 Carbon nanotube (MWCNT) functionalization and electrode modification

MWCNT were purified and functionalized as described elsewhere [17]. First, a given amount of MWCNT in 5 M nitric acid was stirred for 24 h, the solid product was collected on a filter paper and washed successively with Milli-Q water until the filtrate solution reached neutral pH, and dried in an oven at 80 ºC overnight. This pre-treatment was used for removal of impurities derived from the synthetic process such as residues of metal catalysts and amorphous carbon. Nitric acid leads to the creation of some defects in carbon nanotube structures and functionalization by insertion of some negative groups $–COO^-$, improving their conductivity [18,19]. A dispersion of 1.0 % w/v MWCNT prepared in 1.0 % w/v chitosan solution dissolved in 1.0 % v/v acetic acid solution was sonicated for 2 h until a homogeneous dispersion was obtained. A volume of 1 μL of the MWCNT-chitosan dispersion was drop cast two times on

the surface of GCE leaving to dry each time for ~ 60 min at room temperature, before PBCB electrodeposition.

2.4 Electrodeposition of PBCB films on MWCNT/GCE

Ethaline DES, consisting of a 1:2 molar ratio of choline chloride: ethylene glycol was prepared by pre-heating solid choline chloride at 80 ºC in order to evaporate the excess of water, followed by addition of ethylene glycol under stirring and heating up to 100 ºC until a homogeneous and colourless solution was obtained. After cooling down to room temperature, a calculated volume of concentrated HNO_3 (65 %) was added to ethaline DES to obtain a final concentration of 0.5 M of acid, and then BCB was added to give a 0.1 mM BCB monomer solution.

PBCB films were formed in ethaline+HNO_3 in both potentiostatic and potentiodynamic mode on MWCNT/GCE and their electrochemical behaviour was compared. In potentiostatic electropolymerisation mode, the influence of varying the applied potential (0.8 V, 1.0 V or 1.2 V vs. Ag/AgCl), as well as the electrodeposition time (100, 300, 600, 900 s) was studied. PBCB films were also potentiodynamically prepared on MWCNT/GCE by cycling during 30 scans in the potential range from – 0.6 V to +1.0 V vs. Ag/AgCl at 150 mV s^{-1}, as in [15]. For comparison, PBCB films were formed in aqueous solution containing 0.1 mM BCB +0.1 M KNO_3 + 0.1 M PB (pH 7.0), with the same optimized experimental conditions as used in DES ethaline – HNO_3, for both electropolymerisation modes.

2.5 Preparation of choline oxidase (ChOx) biosensor

Choline oxidase (ChOx) was immobilized onto the modified electrode surfaces by cross-linking with glutaraldehyde (GA) and with bovine serum albumin (BSA) as carrier protein. The enzyme solution was prepared by mixing 10 mg BSA with different amounts of ChOx, from 1.0 to 3.5 mg, in 1 mL of 0.1 M PB, pH 7.0. A volume of 1 μL of the enzyme solution containing BSA

was dropped on the modified electrode surfaces, followed by dropping of 1 μL of GA (2.5 %) and was left to dry for 1 h at room temperature. After immobilization, the enzyme-coated electrodes were immersed in buffer solution (pH 7.0) for at least 2 h in order to hydrate the formed membrane and facilitate the diffusion of ionic species. When not in use, the biosensors were stored in buffer solution at 4 °C.

2.6 Enzyme inhibition measurements

Enzyme inhibition for determination of dichlorvos organophosphorus pesticide using the ChOx/PBCB/MWCNT/GCE biosensor was done by fixed potential amperometric measurements in buffer solution. After stabilization of the baseline current, a chosen choline concentration was added and the steady current recorded (I_o). Then, known concentrations of dichlorvos were added to inhibit the enzyme activity and the current was measured (I_1), which is proportional to the concentration of the inhibitor in solution. The degree of inhibition, *I %*, was calculated according to the equation [20]:

$$I\ \% = \frac{I_o - I_1}{I_o} \text{x } 100 \quad (1)$$

3. Results and discussion

Poly(brilliant cresyl blue) films were formed on MWCNT/GCE potentiostatically at a fixed applied potential and potentiodynamically by potential cycling, as described in the experimental section. The following terminology will be used to distinguish the electropolymerisation methods: $PBCB^{PTD}$ (potentiostatic deposition of polymer film) and $PBCB^{PDD}$ (potentiodynamic deposition of polymer film). In both cases, polymerization was carried out in ethaline DES-HNO_3 solutions and in aqueous solution.

The optimized experimental condition for the formation of $PBCB^{PDD}$ films have been reported elsewhere [15]; here, only their electrochemical performance, as well as their morphology studies by SEM, will be shown and discussed for comparison purposes.

3.1 Electrosynthesis of PBCB films

For the preparation of $PBCB^{PTD}$ films in ethaline-HNO_3 solutions, a polymerization solution containing BCB+ethaline+ HNO_3 was used, as described in the experimental section. For the optimisation of this method, the influence of some parameters was investigated such as the composition of the polymerization solutions, applied potential and deposition time.

3.1.1 Influence of applied potential during polymerization

The applied potential used for the potentiostatic, fixed potential, polymer synthesis has a big influence on the amount of polymer film formed. Fig 1A1 shows chronoamperometric curves ($j - t$) of $PBCB_{ethaline}$-HNO_3 film electrodeposition at values of applied potential of 0.8, 1.0 and 1.2 V vs. Ag/AgCl, during 300 s (the $PBCB_{ethaline}$-HNO_3 films did not grow when less positive potentials were employed). The curves show the characteristic profile of potentiostatic polymerization. First, there is a rapid increase in current attributed to double layer charging and oxidation of monomer close to the electrode surface and following this, when the current begins to decay, nucleation takes place accompanied by continuous and gradual polymer growth. The higher initial currents with increasing applied potential reflect a higher rate of nucleation.

An increase in applied potential during potentiostatic polymerization may result in two opposite effects. One is an increase of the polymerization rate as mentioned above. The other effect is the enhancement of degradation processes by overoxidation at more positive potentials,

influencing the polymer's electrochemical activity, equivalent to the loss of a certain amount of polymer. That this happens is shown by the lower peak currents in the CV of the $PBCB_{ethaline}$-HNO_3 films, Fig 1A2, obtained at 1.0 and 1.2 V vs. For 1.2 V polymerisation potential, the peak currents in the CV profile are not as well-defined as for 1.0 V. Similar behaviour has been reported for other polymers e.g. PEDOT and polypyrrole [21,22].

The surface coverage (Γ) of MWCNT/GCE was estimated using the equation [23]:

$$\Gamma = Q / nFA \quad (2)$$

where Γ is the surface concentration (mol cm^{-2}), Q is the charge obtained by integrating the CV over the potential range of the more well-defined cathodic peak (I_c), ascribed to polymer formation, n (=2) is the number of electrons transferred, F is the Faraday constant (96485 C mol^{-1}) and A is the electrode geometric surface area (0.00785 cm^2). The values of (Γ) were calculated to be: 3.72 x 10^{-7} < 4.23 x 10^{-7} < 5.05 x 10^{-7} mol cm^{-2}, for $PBCB_{ethaline}$-HNO_3 electrodeposited at 1.2, 1.0 and 0.8 V respectively. The electrochemical response of the $PBCB_{ethaline}$-HNO_3 films obtained at 0.8 V vs. Ag/AgCl was higher and was chosen as the best.

3.1.2 Influence of deposition time

The influence of the deposition time on the amount of $PBCB_{ethaline}$-HNO_3 film formed was also assessed. $PBCB_{ethaline}$-HNO_3 films were electrodeposited at 0.8 V vs. Ag/AgCl, as previously optimized, Fig. 1B1, and deposition was stopped after periods of 100, 300, 600 and 900 s). The CV profile of the polymer films, Fig 1B2, all present two redox couples (I_a/I_c and II_a/II_c), in which increasing the deposition time from 100 to 300 s, a significantly greater amount of polymer film is deposited, as revealed by higher peak currents. For longer deposition times of 600 and 900 s, the peak currents have almost the same magnitude as for 300s, indicating little further deposition. The surface coverage (Γ) was calculated to be 2.15 x 10^{-7}, 5.80 x 10^{-7}, 5.82

x 10^{-7}, and 5.85x 10^{-7} mol cm^{-2} for 100, 300, 600, and 900 s deposition time, respectively. Thus, a deposition time of 300 s was chosen as optimum.

3.2 Influence of the electrodeposition mode on PBCB film morphology

Fig. 2 shows SEM images of PBCB films on MWCNT-modified carbon film electrodes produced under the optimized conditions described previously. The morphology of the PBCB films depends considerably on the electropolymerisation method and the medium in which it was carried out.

In aqueous medium and for the $PBCB_{aq}^{PDD}$ film, Fig 2A, only a small amount of polymer is electrodeposited with incomplete coverage. The overall morphology of the MWCNT surface did not change, revealed by the presence of some exposed MWCNT bundles in the nanocomposite film, as also reported in [24–26]. Conversely, the $PBCB_{aq}^{PTD}$ film, Fig 2B, revealed a thicker morphology covering all MWCNT bundles indicating a greater polymer film mass, besides the presence of some globular-like shape nanostructures. The difference in the morphologies of the PBCB films may be attributed to a secondary nucleation process on the previously formed polymer, often found for potentiostatic electrodeposition [27].

Polymer films formed in ethaline DES-HNO_3 by the two electropolymerisation methods present a more compact surface than PBCB films prepared in aqueous solution. However, in the case of $PBCB_{ethaline}$-HNO_3^{PDD} film, Fig 2C, some irregularities are observed with a rougher surface. For the $PBCB_{ethaline}$-HNO_3^{PTD}, Fig 2D, a completely smooth and uniform surface was obtained. The structures with greater roughness observed for films grown by potentiodynamic mode are most likely associated with the effects of the entry and expulsion of counter ions during each voltammetric cycle. Under potentiostatic conditions, the polymer grows continuously at a faster rate and the counter ions are accumulated throughout the whole polymerization procedure and.

as a result, a smoother surface is formed. These results are in agreement with the observations of Zhang et al [27].

*3.3. Application of ChOx/PBCB$_{aq}$ and ChOx/*PBCB$_{ethaline}$-HNO_3 *biosensor to choline detection*

Choline biosensors were prepared by immobilising choline oxidase on the four types of optimised PBCB modified MWCNT/GCE i.e. PBCB formed by potentiostatic and potentiodynamic modes and, for each, prepared in DES or aqueous media, as discussed above. Amperometric measurements of choline for the different biosensor configurations were carried out in 0.1 M PB solution, pH 7.0, at an applied potential of -0.3 V vs. Ag/AgCl as optimized in [28], in which 3.5 mg mL^{-1} ChOx was used as enzyme loading. A typical chronoamperogram for the response to choline at ChOx/PBCB$_{ethaline}$-HNO_3^{PTD}/MWCNT/GCE is shown in Fig 3A, evidencing an increase of the change in cathodic current with increase of choline concentration for all biosensor assemblies tested. Fig 3B displays calibration plots for all biosensor configurations with the corresponding analytical parameters summarized in Table 1.

As observed, the highest sensitivity of 107 μA cm^{-2} mM^{-1} and lowest limit of detection (LoD) 1.55 μM was reached at the ChOx/PBCB$_{ethaline}$-HNO_3^{PTD}/MWCNT/GCE biosensor, following the linear regression equation: $\Delta j(\mu A\ cm^{-2})$ = 0.61 + 0.11 [choline](μM). For the ChOx/PBCB$_{ethaline}$-HNO_3^{PDD}/MWCNT/GCE biosensor the sensitivity was 77 μA cm^{-2} $mM^{-1}$and the LoD was 1.91 μM, where $\Delta j(\mu A\ cm^{-2})$ = 0.35 + 0.077 [choline](μM). The ChOx/PBCB$_{aq}^{PTD}$/MWCNT/GCE biosensor presented a sensitivity of 41 μA cm^{-2} mM^{-1} and LoD of 2.43 μM, with $\Delta j(\mu A\ cm^{-2})$ = 0.69 + 0.041[choline](μM). Finally, the ChOx/PBCB$_{aq}$ ^{PTD}/MWCNT/GCE biosensor had the lowest sensitivity of 21 μA cm^{-2} mM^{-1} and LoD 3.41 μM, with $\Delta j(\mu A\ cm^{-2})$ = 0.05 + 0.021 [choline](μM).

The ChOx/PBCB$_{ethaline}$-HNO_3^{PDD}/MWCNT/GCE biosensor has the best or similar electrochemical performance compared with some of the most recent ChOx biosensors for

choline determination found in the literature. For instance, an amperometric choline biosensor consisting of choline oxidase immobilised on a PB–$FePO_4$ nanocomposite modified GCE, exhibited a sensitivity of 75.2 μA mM^{-1} cm^{-2} and LoD of 0.4μM [29]. Yang et al. [30], developed a bi-enzymatic biosensor for choline determination based on ChOx and horseradish peroxidase (HRP) immobilized on poly(thionine) film modified carbon paste electrodes; the sensitivity of this biosensor was 0.75 μA mM^{-1} cm^{-2} and LoD was 3.0 μM. Rahimi et al. [31], proposed a choline biosensor by immobilization of ChOx on RTIL/NH_2-MWCNT/GCE; the sensitivity being 125.8 μA mM^{-1} cm^{-2} and with LoD of 3.85 μM. Yu et al. [32], also developed a biosensor based on the immobilization of ChOx on manganese dioxide (MnO_2) nanoparticle modified GCE, which exhibited a sensitivity of 7.86 8 μA mM^{-1} and LoD of 5.0 μM. Thus, ChOx/$PBCB_{ethaline}$-HNO_3^{PDD}/MWCNT/GCE was chosen as the best biosensor configuration for inhibition studies.

3.4. Inhibition measurements

3.4.1 Influence of the pH, applied potential and enzyme loading

The dependence of the degree of inhibition on pH was assessed in the pH range from 6.0 to 8.0. The response of the biosensor to 20 nM dichlorvos, in the presence of 0.5 mM choline varied significantly with pH as illustrated in Fig 4A. The inhibition measurements were initially carried out at an applied potential of -0.3 V vs. Ag/AgCl and 3.8 mg mL^{-1} enzyme loading. As can be observed, the change in amperometric response due to inhibition rises with increase of pH from 6.0 to 7.0, where the maximum is reached, and then decreases again. Thus, PB solution pH = 7.0 was chosen for further inhibition experiments.

The influence of the applied potential was also assessed by measuring the amperometric response to 20 nM dichlorvos using the same concentration of choline and ChOx at fixed

potentials ranging from -0.4 to + 0.2 V vs. Ag/AgCl, Fig 4B. The response to dichlorvos increases from -0.4 to -0.3 V vs. Ag/AgCl and then decreases as the applied potential was shifted to less negative potential values. The highest degree of inhibition is exhibited at -0.3 vs. Ag/AgCl, which was chosen as optimum.

The enzyme concentration can also influence the enzymatic activity under inhibition conditions. The effect of 0.5 mM choline in the presence of successive additions of dichlorvos was tested by measuring the activity for three different concentration of choline oxidase (ChOx) (1.0, 2.5 and 3.5 mg mL^{-1}) immobilized on $PBCB_{ethaline}$-HNO_3^{PTD} MWCNT/GCE. Fig 4B shows calibration plots and an increase of the sensitivity to inhibitor is clearly observed when the ChOx concentration was increased: 628, 764 and 950 μA cm^{-2} μM^{-1} for 1.0, 2.5 and 3.5 mg mL^{-1} enzyme loading, respectively. The highest sensitivity was achieved for 3.5 mg mL^{-1} ChOx immobilised on $PBCB_{ethaline}$-HNO_3^{PTD}MWCNT/GCE and therefore was chosen as optimum and used in further enzyme inhibition experiments.

3.4.2 Mechanism of inhibition

To study the mode of interaction between the dichlorvos and the active site of ChOx, a new and simple graphical method for the determination of reversible inhibition type was employed [16]. This is based on the effect of different enzyme substrate concentrations on I_{50} (concentration of inhibitor necessary to inhibit 50 % of the initial response to the substrate). Three choline concentrations, namely 0.3, 0.5 and 1.0 mM, were used, as shown in Fig. 5A. In this method, if the value of I_{50} decreases whilst the substrate concentration increases, and maximum inhibition increases, then the inhibition mechanism is uncompetitive, as happens in this work after successive additions of known concentrations of dichlorvos in the presence of different concentrations of choline, Fig 5A.

The mechanism of inhibition was also evaluated from the classical Dixon and Cornish-Bowden plots. The Dixon plot, Fig 5B, showed parallel lines and Cornish-Bowden plots, Fig 5C, showed an intersection of the lines on the left side of the y-axis, above the inhibitor axis, both in agreement with uncompetitive inhibition mechanism.

The enzyme inhibition constant (K_i) was estimated by equation 3, from the relationship between I_{50} and K_i, for an uncompetitive inhibition mechanism, as proposed by Amine et al [16].

$$\frac{I_{50}}{K_i} = \left(1 + \frac{K_m}{[S]}\right) \quad (3)$$

where K_m = 39.2 μM, is the Michaelis-Menten constant of the enzyme without the presence of inhibitor and [S] = 0.5 mM, is the substrate concentration. The enzyme inhibition constant (K_i) was calculated to be 19.8 nM, close to the value obtained from the intercepts of the curves of the Cornish-Bowden plots, 19.2 nM, corresponding to good agreement between the two approaches.

3.4.3 Analytical performance of the inhibition biosensor

Amperometric measurements of dichlorvos at the $PBCB_{ethaline}$-HNO_3^{PTD}MWCNT/GCE were carried out in 0.1 M PB, pH 7.0 at an applied potential of - 0.3 V vs. Ag/AgCl, as previously optimized. As seen above, the concentration of the enzyme substrate can greatly influence on the degree of inhibition over each inhibitor aliquots injected. Thus, the concentration of the enzyme substrate needs to be carefully chosen. Independently of the mechanism of inhibition, a higher concentration of the enzyme substrate can lead to a decrease of enzyme inhibition by the inhibitor. On the other hand, when the concentration of the substrate is low, a saturation of the enzyme activity is observed in the presence of low inhibitor concentrations, compromising its response. To minimize these effects, an intermediate value of 0.5 mM choline, Fig 5A, was chosen for calibration plots.

In some inhibition studies, the limit of detection is calculated based on a signal-to-noise ratio of 3 (S/N=3) and others consider I_{10} value (concentration necessary for 10 % inhibition of the initial response of the substrate). The LoD and I_{10} were calculated to be 1.59 and 9.96 nM respectively. From the linear response between 2.5 and 60 nM, the following equation was obtained: Δj (μA cm^{-2}) = -1.47+1.15 [dichlorvos] (nM). Independently of the method of calculation, the present biosensor exhibited the lowest of the detection limits reached until now for dichlorvos detection, see Table 2. Besides this, the novel ChOx/$PBCB_{ethaline}$-HNO_3^{PTD} /MWCNT/GCE biosensor has several advantages, such as easy preparation, fast response, and low applied potential compared with the other biosensors for dichlorvos detection in Table 2. Furthermore, it did not require any kind of special procedure for restoring the ChOx activity such as immersion of the electrodes in buffer solution and/or successive potential scans, to restore the original activity.

Additional experiments were also carried out for direct detection of dichlorvos by square wave voltammetry (results not shown). The peak current increased linearly with dichlorvos concentration in the range from 0.8 to 30 μM. The linear equation was calculated as Δj (μA cm^{-2}) = 0.14+0.24 [dichlorvos] (μM) with a limit of detection of 0.6 μM. However, the limit of detection achieved is not as low as the nanomolar detection limit obtained by the enzyme inhibition method, that can quantify concentration values less than those considered hazardous for living organisms.

3.4.4 Selectivity

To identify potential interferents and selectivity of the ChOx/$PBCB_{ethaline}$-HNO_3^{PTD} /MWCNT/GCE biosensor, interference studies were carried out in the presence of some interfering species which are known to be able to inhibit enzyme activity and which could be present in waters or agricultural produce. These were trace metal ions (Cu^{2+}, Fe^{2+}, Ni^{2+}, Co^{2+},

Cd^{2+}, Hg^{2+} and Cr^{VI}) and the pesticides cyanazin and terbutryn, Fig 8. The inhibition caused by each interferent was evaluated in independent experiments in relation to the initial response to 0.5 mM choline at an applied potential of – 0.3 V vs. Ag/AgCl, as previously optimized; the concentration of each interferent injected in the electrochemical cell was 100 nM. The degree of inhibition for all interferents tested had no significant influence over the initial response of choline, less than 5%. In general, the ChOx/$PBCB_{ethaline}$-HNO_3^{PTD}/MWCNT/GCE biosensor exhibited good selectivity towards the dichlorvos response, which suggests its use for monitoring trace dichlorvos in agricultural produce, and for monitoring in water.

3.4.5 Repeatability and stability

Repeatability and stability are also important factors for practical application of enzyme biosensors. Good repeatability with a relative standard deviation (RSD) less than 5.0 % was obtained by evaluation of five different ChOx/$PBCB_{ethaline}$-HNO_3^{PTD}/MWCNT/GCE biosensors by the injection of the same concentration of dichlorvos, 20 nM. Additionally, the stability of ChOx biosensor was assessed by monitoring the 0.5 mM choline amperometric response after 10 consecutive injections of 20 nM dichlorvos every day for 20 days. After 20 days the choline response still retained 95.6 % of the initial response, demonstrating excellent stability of the biosensor.

3.4.6 Application to beverages

To evaluate the feasibility of the biosensor for environmental monitoring, application to the determination of dichlorvos in orange juice by the standard addition method was examined. Prior to measurements, the extracted orange juice was strained through a fine mesh sieve. Afterwards, the orange juice was centrifuged at 14,000 rpm for 20 min, then the supernatants

were collected and kept at 4 °C before use. The juice samples, after pre-treatment, were spiked with three known concentration of dichlorvos, Table 3. The average recovery was in the range of 99.7 – 103.2%, which indicates the efficient applicability of the biosensor for practical analysis.

4. Conclusions

Ethaline DES permitted the formation of polymer nanostructured films with superior electrochemical performance compared with films formed in aqueous solution in both potentiostatic and potentiodynamic polymerization modes. SEM studies demonstrated that morphology is greatly dependent on the composition of the polymerization solutions and electrodeposition mode, the polymer films produced from ethaline-HNO_3 in potentiostatic mode having a smoother and more compact nanostructure. These were found to be the best for the construction of a choline biosensor and its application to determine dichlorvos by enzyme inhibition. The mechanism of dichlorvos inhibition was found to be uncompetitive. The novel enzyme inhibition biosensor exhibited superior analytical parameters to other comparable biosensors. It has the lowest limits of detection, with good selectivity and stability, compared with those in the literature and was successfully applied to dichlorvos detection in orange juice with excellent recoveries. The results demonstrate that the novel biosensor can be adopted as a promising analytical tool for monitoring trace pesticides in agricultural produce and waters.

Acknowledgements

The authors thank Fundação para a Ciência e a Tecnologia (FCT), Portugal, projects PTDC/QEQ-QAN/2201/2014, in the framework of Project 3599-PPCDT, and UID/EMS/00285/2013 (both co-financed by the European Community Fund FEDER). WS thanks the Conselho Nacional de Desenvolvimento Científico e Tecnológico (CNPq), Brazil

for a doctoral fellowship, 232979/2014-6 and MEG thanks FCT for a postdoctoral fellowship SFRH/BPD/103103/2014.

5. References

[1] D. Song, Y. Li, X. Lu, M. Sun, H. Liu, G. Yu, F. Gao, Palladium-copper nanowires-based biosensor for the ultrasensitive detection of organophosphate pesticides, Anal. Chim. Acta 982 (2017) 168–175.

[2] Q. Lang, L. Han, C. Hou, F. Wang, A. Liu, A sensitive acetylcholinesterase biosensor based on gold nanorods modified electrode for detection of organophosphate pesticide, Talanta 156 (2016) 34-41.

[3] Q. Shi, Y. Teng, Y. Zhang, W. Liu, Rapid detection of organophosphorus pesticide residue on Prussian blue modified dual-channel screen-printed electrodes combing with portable potentiostat, Chinese Chem. Lett. 29 (2018) 1379-1382.

[4] C. Grasshoff, H. Thiermann, T. Gillessen, T. Zilker, L. Szinicz, Internal standard high-performance liquid chromatography method for the determination of obidoxime in urine of organophosphate poisoned patients, J. Chromatogr. B 753 (2001) 203–208.

[5] D. Chen, Y. Jiao, H. Jia, Y. Guo, X. Sun, X. Wang, J. Xu, Acetylcholinesterase biosensor for chlorpyrifos detection based on multi-walled carbon nanotubes-SnO_2 chitosan nanocomposite modified screen-printed electrode, Int. J. Electrochem. Sci. 10 (2015) 10491–10501.

[6] A.R. Fontana, A.B. Camargo, J.C. Altamirano, Coacervative microextraction ultrasound-assisted back-extraction technique for determination of organophosphates pesticides in honey samples by gas chromatography-mass spectrometry, J. Chromatogr. A 1217 (2010) 6334-6341.

[7] K. Sipa, M. Brycht, A. Leniart, P. Urbaniak, A. Nosal-Wiercińska, B. Pałecz, S. Skrzypek, β–Cyclodextrins incorporated multi-walled carbon nanotubes modified electrode for the voltammetric determination of the pesticide dichlorophen, Talanta 176 (2018) 625–634.

[8] J.C. Vidal, S. Esteban, J. Gil, J.R. Castillo, A comparative study of immobilization methods of a tyrosinase enzyme on electrodes and their application to the detection of dichlorvos organophosphorus insecticide, Talanta 68 (2006) 791-799.

[9] J. G. Ayenimo, S.B. Adeloju, Rapid amperometric detection of trace metals by inhibition of an ultrathin polypyrrole-based glucose biosensor, Talanta 148 (2016) 502–510.

[10] M.M. Barsan, M.E. Ghica, C.M.A. Brett, Electrochemical sensors and biosensors based on redox polymer/carbon nanotube modified electrodes: A review, Anal. Chim. Acta 881 (2015) 1–23.

[11] M.M. Barsan, C.M.A. Brett, Recent advances in layer-by-layer strategies for biosensors incorporating metal nanoparticles, TrAC - Trends Anal. Chem. 79 (2016) 286–296.

[12] K.P. Prathish, M.M. Barsan, D. Geng, X. Sun, C.M.A. Brett, Chemically modified graphene and nitrogen-doped graphene: Electrochemical characterisation and sensing

applications, Electrochim. Acta 114 (2013) 533-542.

[13] D. Di Marino, M. Shalaby, S. Kriescher, M. Wessling, Corrosion of metal electrodes in deep eutectic solvents, Electrochem. Commun. 90 (2018) 101-105.

[14] L.I.N. Tomé, V. Baião, W. da Silva, C.M.A. Brett, Deep eutectic solvents for the production and application of new materials, Appl. Mater. Today 10 (2018) 30–50.

[15] W. da Silva, M.E. Ghica, C.M.A. Brett, Novel nanocomposite film modified electrode based on poly(brilliant cresyl blue) - deep eutectic solvent/carbon nanotubes and its biosensing applications, Electrochim. Acta 317 (2019) 766-777.

[16] A. Amine, L. El Harrad, F. Arduini, D. Moscone, G. Palleschi, Analytical aspects of enzyme reversible inhibition, Talanta 118 (2014) 368–374.

[17] M.E. Ghica, R. Pauliukaite, O. Fatibello-Filho, C.M.A. Brett, Application of functionalised carbon nanotubes immobilised into chitosan films in amperometric enzyme biosensors, Sens. Actuators B: Chem. 142 (2009) 308–315.

[18] P. Papakonstantinou, R. Kern, L. Robinson, H. Murphy, J. Irvine, E. McAdams, J. McLaughlin, T. McNally, Fundamental electrochemical properties of carbon nanotube electrodes, fullerenes nanotube. Carbon Nanostructures 13 (2005) 91–108.

[19] N.S. Lawrence, R.P. Deo, J. Wang, Comparison of the electrochemical reactivity of electrodes modified with carbon nanotubes from different sources, Electroanalysis 17 (2005) 65-72.

[20] B. Elsebai, M.E. Ghica, M.N. Abbas, C.M.A. Brett, Catalase based hydrogen peroxide biosensor for mercury determination by inhibition measurements, J. Hazard. Mater. 340 (2017) 344–350.

[21] X. Du, Z. Wang, Effects of polymerization potential on the properties of electrosynthesized PEDOT films, Electrochim. Acta 48 (2003) 1713–1717.

[22] N.C.T. Martins, T. Moura e Silva, M. F. Montemor, J.C.S. Fernandes, M.G.S. Ferreira, Electrodeposition and characterization of polypyrrole films on aluminium alloy 6061-T6, Electrochim. Acta 53 (2008) 4754–4763.

[23] E. Laviron, General expression of the linear potential sweep voltammogram in the case of diffusionless electrochemical systems, J. Electroanal. Chem. 101 (1979) 19–28.

[24] H. Yi, D. Zheng, C. Hu, S. Hu, Functionalized multiwalled carbon nanotubes through in situ electropolymerization of brilliant cresyl blue for determination of epinephrine, Electroanalysis 20 (2008) 1143–1146.

[25] H. Liu, G. Wang, J. Hu, D. Chen, W. Zhang, B. Fang, Electrocatalysis and determination of uracil on polythionine/multiwall carbon nanotubes modified electrode, J. Appl. Polym. Sci. 107 (2008) 3173–3178.

[26] Y. Xu, X. Zhang, Y. Wang, P. He, Y. Fang, Enhancement of electrochemical capacitance of carbon nanotubes by polythionine modification, Chinese J. Chem. 28 (2010) 417–421.

[27] E. Kim, N. Kang, J.-J. Moon, M. Choi, A comparative study of potentiodynamic and potentiostatic modes in the deposition of polyaniline, Bull. Korean Chem. Soc. 37 (2016)

1445–1452.

[28] H.S. Magar, M.E. Ghica, M.N. Abbas, C.M.A. Brett, A novel sensitive amperometric choline biosensor based on multiwalled carbon nanotubes and gold nanoparticles, Talanta 167 (2017) 462–469.

[29] H. Zhang, Y. Yin, P. Wu, C. Cai, Indirect electrocatalytic determination of choline by monitoring hydrogen peroxide at the choline oxidase-prussian blue modified iron phosphate nanostructures, Biosens. Bioelectron. 31 (2012) 244–250.

[30] M. Yang, Y. Yang, Y. Yang, G. Shen, R. Yu, Bienzymatic amperometric biosensor for choline based on mediator thionine in situ electropolymerized within a carbon paste electrode, Anal. Biochem. 334 (2004) 127–134.

[31] P. Rahimi, H. Ghourchian, S. Sajjadi, Effect of hydrophilicity of room temperature ionic liquids on the electrochemical and electrocatalytic behaviour of choline oxidase, Analyst 137 (2012) 471–475.

[32] G. Yu, Q. Zhao, W. Wu, X. Wei, Q. Lu, A facile and practical biosensor for choline based on manganese dioxide nanoparticles synthesized in-situ at the surface of electrode by one-step electrodeposition, Talanta 146 (2016) 707–713.

[33] H.F. Cui, W.W. Wu. M.M. Li, X. Song, Y. Lv, T.T. Zhang, A highly stable acetylcholinesterase biosensor based on chitosan-TiO_2-graphene nanocomposites for detection of organophosphate pesticides, Biosens. Bioelectron. 99 (2018) 223–229.

[34] S. Wu, F. Huang, X. Lan, X. Wang, J. Wang, C. Meng, Electrochemically reduced graphene oxide and Nafion nanocomposite for ultralow potential detection of organophosphate pesticide, Sens. Actuators B: Chem. 177 (2013) 724–729.

[35] X.A. Zhang, H.H. Jia, X.F. Wang, H.L. Zhang, H.W. Yin, S.L. Chang, J.F. Wang, W.J. Wu, Biosensors based on acetylcholinesterase immobilized on mesoporous silica thin films, Chinese Sci. Bull. 54 (2009) 3023–3028.

[36] M. Shi, J. Xu, S. Zhang, B. Liu, J. Kong, A mediator-free screen-printed amperometric biosensor for screening of organophosphorus pesticides with flow-injection analysis (FIA) system, Talanta 68 (2006) 1089–1095.

Fig. 1 Potentiostatic formation of PBCB films on MWCNT/GCE from solutions containing 0.1 mM BCB in 0.5 M HNO_3 – ethaline (A1) at different applied potentials (0.8, 1.0 and 1.2 V vs. Ag/AgCl) for 300 s. (B1) at 0.8 V for 900 s deposition time. CVs of PBCB films in 0.1 M PB (pH 7.0) at 50 mV s^{-1} formed (A2) at different applied potentials, (B2) during different electropolymerisation times.

Fig. 2 SEM micrographs of PBCB films on MWCNT/CFE electrodeposited in: (A) 0.1 M KNO_3 + 0.1 M PB (pH 7.0) at 150 mVs^{-1}; (B) 0.1 M KNO_3 + 0.1 M PB (pH 7.0) at 0.8 V vs. Ag/AgCl during 300 s; (C) ethaline + 0.5 M HNO_3 at 150 mVs^{-1}; (D) ethaline + 0.5 M HNO_3 at 0.8 V vs. Ag/AgCl during 300 s.

Fig. 3 (A) Amperometric response of ChOx/ $PBCB_{ethaline}$-HNO_3^{PTD} biosensor to choline. (B) Calibration curves for choline in 0.1 M PB (pH 7.0) at −0.30 V for: (a) ChOx/ $PBCB_{ethaline}$-HNO_3^{PTD}/MWCNT/GCE biosensor; (b) ChOx/$PBCB_{ethaline}$-HNO_3^{PDD}/MWCNT/GCE biosensor; (c) ChOx/$PBCBaq^{PTD}$/MWCNT/GCE biosensor; (d) ChOx/$PBCBaq^{PDD}$/ MWCNT/GCE biosensor

Fig. 4 (A) Influence of (A1) pH and (A2) applied potential on the amperometric response to 20 nM dichlorvos in 0.1 M PB at ChOx/$PBCB_{ethaline}$-HNO_3^{PTD}/MWCNT/GCE biosensor in the presence of 0.5 mM choline. (B) Calibration plots for the determination of dichlorvos in 0.1 M PB pH 7.0 for three different ChOx concentrations in the presence of 0.5 mM choline. Applied potential - 0.3 V vs Ag/AgCl.

Fig. 5 (A) Plots for determination of the mechanism of inhibition of dichlorvos in 0.1 M PB (pH 7.0), according to [16], for three different concentrations of choline. (B) Cornish-Bowden (B1) and Dixon (B2) plots for three different concentrations of choline. Applied potential -0.3 V vs. Ag/AgCl.

Fig. 6 Inhibition caused at ChOx/$PBCB_{ethaline}$-HNO_3^{PTD}/MWCNT/GCE by the presence of different interferents in 0.1 M PB (pH 7.0) in the presence of 0.5 mM choline at applied potential - 0.3 V vs. Ag/AgCl. Concentration of interferents: 100 nM.

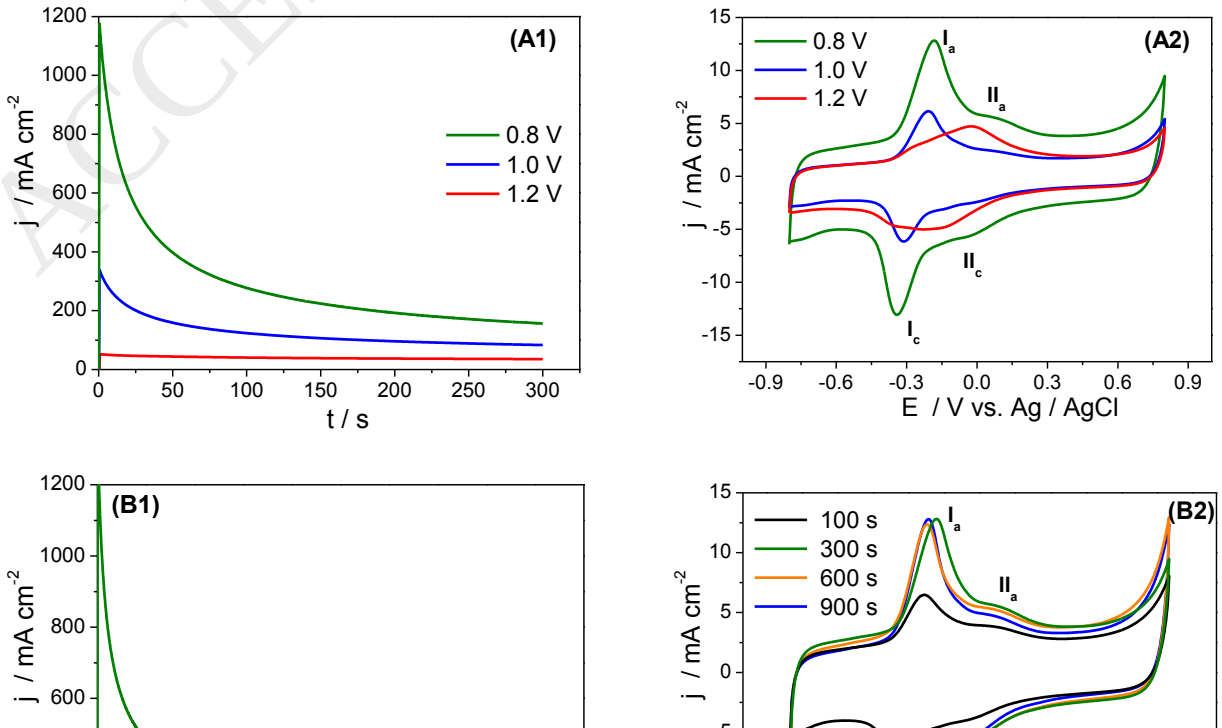

Fig 1 Potentiostatic formation of PBCB films on MWCNT/GCE from solutions containing 0.1 mM BCB in 0.5 M HNO_3 – ethaline (A1) at different applied potentials (0.8, 1.0 and 1.2 V vs. Ag/AgCl) for 300 s. (B1) at 0.8 V for 900 s deposition time. CVs of PBCB films in 0.1 M PB (pH 7.0) at 50 mV s^{-1} formed (A2) at different applied potentials, (B2) during different electropolymerisation times.

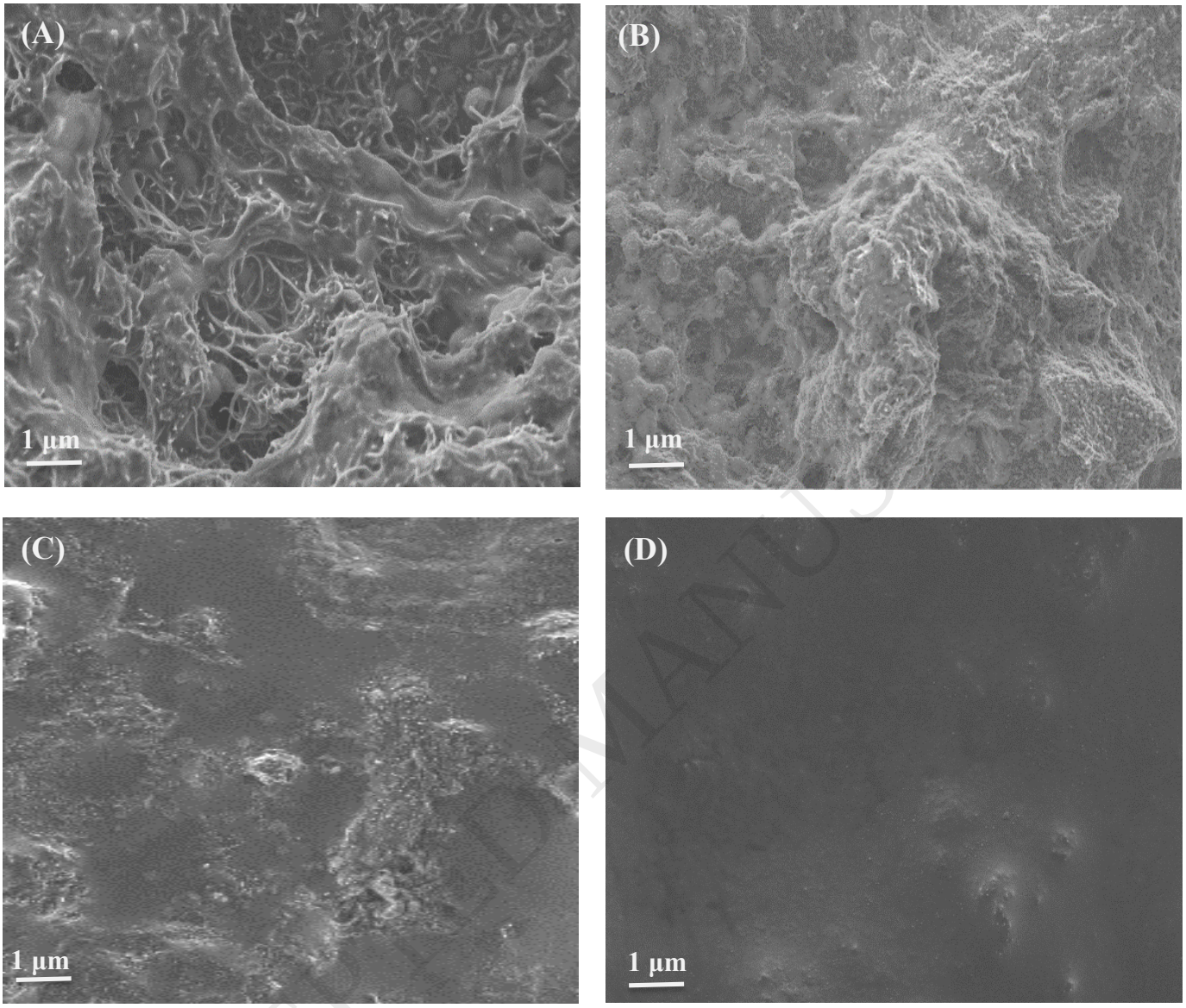

Fig. 2 SEM micrographs of PBCB films on MWCNT/CFE electrodeposited in: (A) 0.1 M KNO_3 + 0.1 M PB (pH 7.0) at 150 mVs^{-1}; (B) 0.1 M KNO_3 + 0.1 M PB (pH 7.0) at 0.8 V vs. Ag/AgCl during 300 s; (C) ethaline + 0.5 M HNO_3 at 150 mVs^{-1}; (D) ethaline + 0.5 M HNO_3 at 0.8 V vs. Ag/AgCl during 300 s.

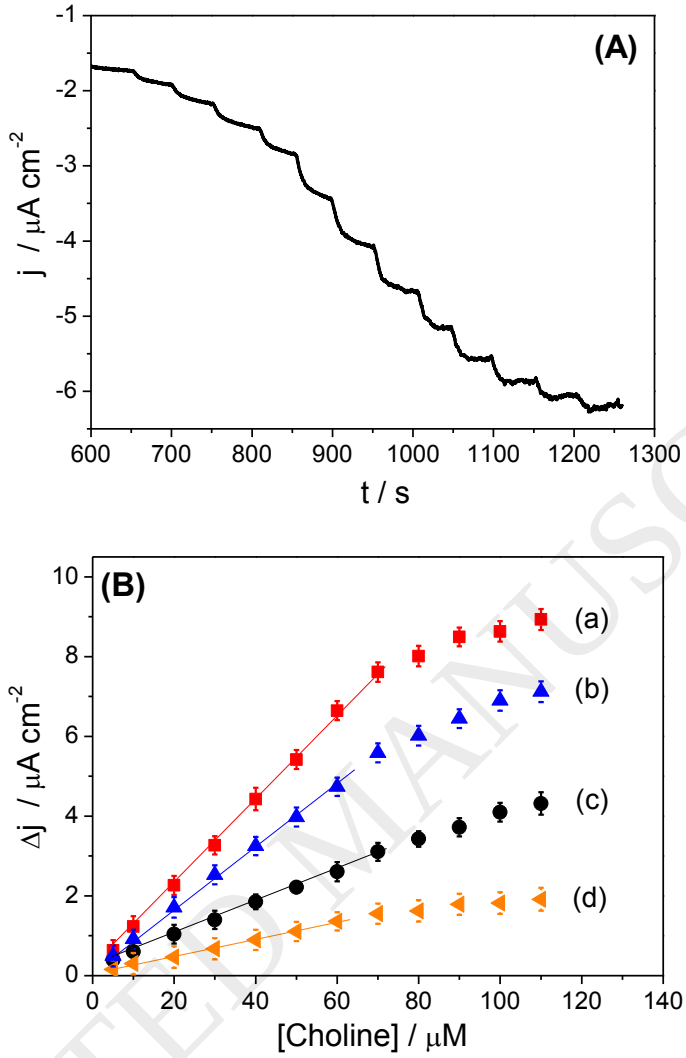

Fig. 3 (A) Amperometric response of ChOx/ $PBCB_{ethaline}$-HNO_3^{PTD} biosensor to choline. (B) Calibration curves for choline in 0.1 M PB (pH 7.0) at −0.30 V for: (a) ChOx/ $PBCB_{ethaline}$-HNO_3^{PTD}/MWCNT/GCE biosensor; (b) ChOx/$PBCB_{ethaline}$-HNO_3^{PDD}/MWCNT/GCE biosensor; (c) ChOx/$PBCBaq^{PTD}$/MWCNT/GCE biosensor; (d) ChOx/$PBCBaq^{PDD/}$ MWCNT/GCE biosensor.

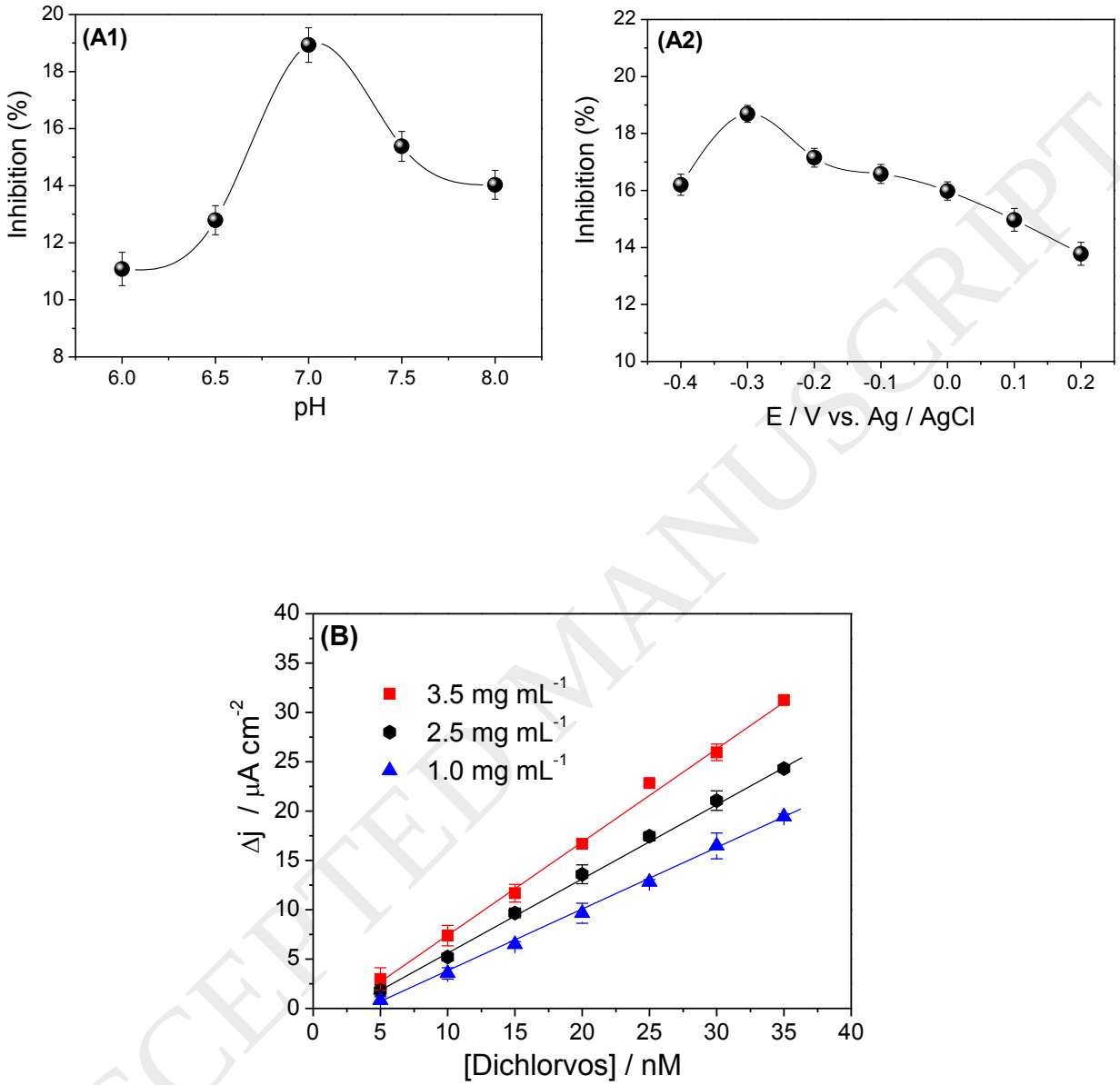

Fig. 4 (A) Influence of (A1) pH and (A2) applied potential on the amperometric response to 20 nM dichlorvos in 0.1 M PB at ChOx/PBCB$_{ethaline}$-HNO$_3^{PTD}$/MWCNT/GCE biosensor in the presence of 0.5 mM choline. (B) Calibration plots for the determination of dichlorvos in 0.1 M PB pH 7.0 for three different ChOx concentrations in the presence of 0.5 mM choline. Applied potential - 0.3 V vs Ag/AgCl.

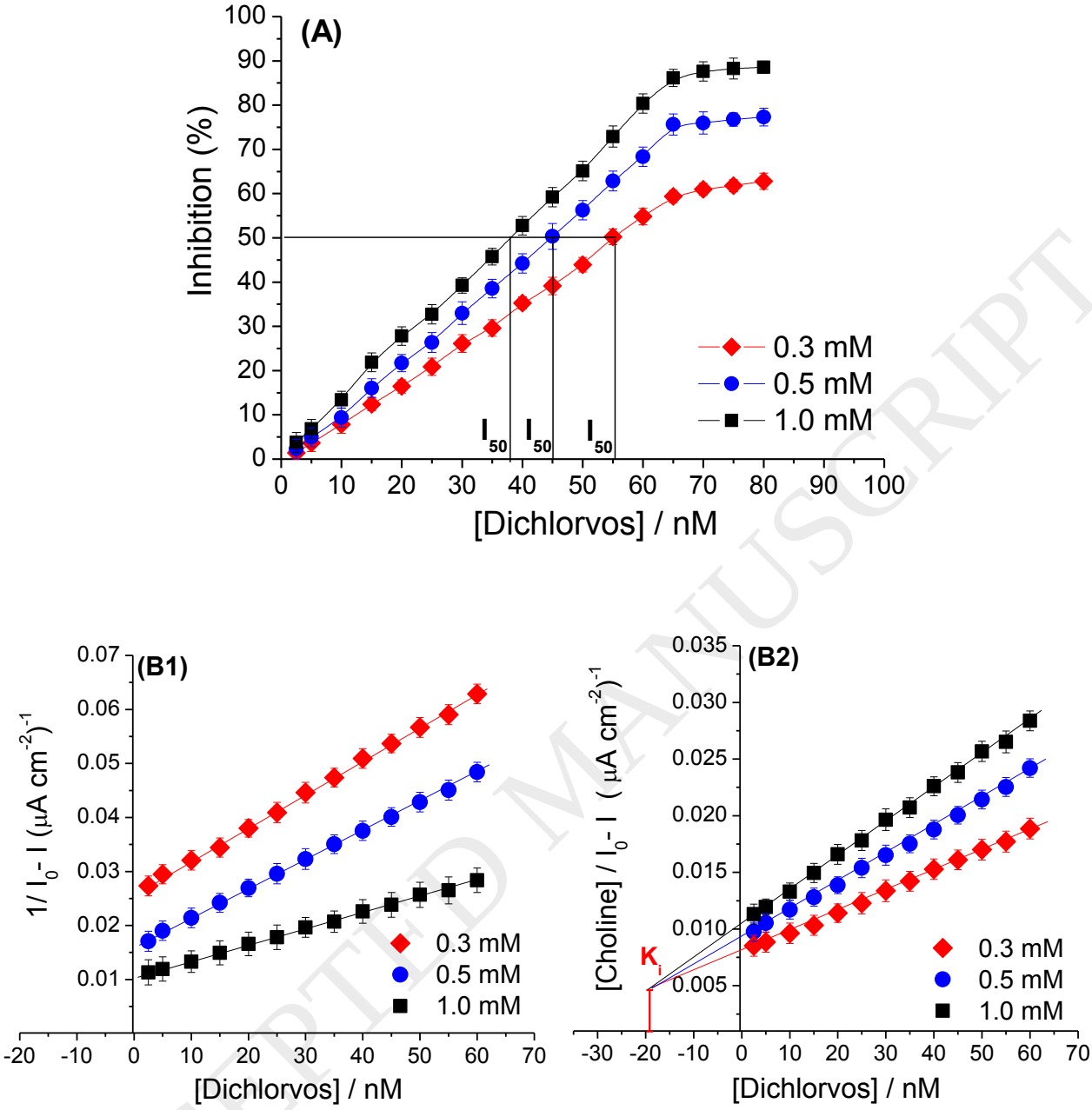

Fig. 5 (A) Plots for determination of the mechanism of inhibition of dichlorvos in 0.1 M PB (pH 7.0), according to [16], for three different concentrations of choline. (B) Cornish-Bowden (B1) and Dixon (B2) plots for three different concentrations of choline. Applied potential -0.3 V vs. Ag/AgCl.

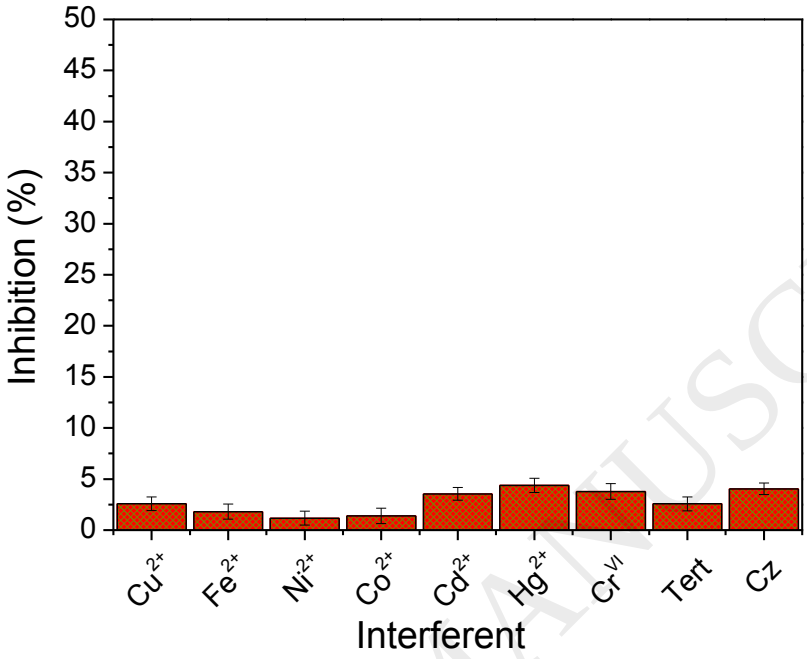

Fig 6 Inhibition caused at ChOx/PBCB$_{ethaline}$-HNO$_3^{PTD}$/MWCNT/GCE by the presence of different interferents in 0.1 M PB (pH 7.0) in the presence of 0.5 mM choline at applied potential - 0.3 V vs. Ag/AgCl. Concentration of interferents: 100 nM

Table 1. Comparative analytical performance of different biosensor configurations to choline

Biosensor Configuration on MWCNT/GCE	LOD / µM	Sensitivity / µA cm^{-2} mM^{-1}
ChOx/PBCBaq ^{PDD}	3.41	21
ChOx/PBCBaq ^{PTD}	2.43	41
ChOx/ PBCB$_{ethaline}$-HNO$_3^{PDD}$	1.91	77
ChOx/ PBCB$_{ethaline}$-HNO$_3^{PTD}$	1.55	107

*PDD - polymer films electrodeposited by potential cycling, 30 cycles

^{*PTD} - polymer films electrodeposited at fixed potential: 0.8 V during 300 s

Table 2. Comparison of the analytical performance of the ChOx/PBCB$_{ethaline}$-HNO$_3^{PTD}$ for dichlorvos determination with other inhibition biosensor configurations.

Biosensor configuration	Mode of detection	Applied potential and pH	Linear range / nM	Detection limit / nM	method	Ref.
AChE/CS@TiO_2-CS/rGO/GCE	Differential pulse voltammetry	E_p ~ 0.65 V vs. (Ag/AgCl), PB (pH 7.4)	36 - 22.6 x10^3	29	incubation	[33]
AChE–Er-GRO–Nafion/GCE	Amperometry	0.5 V vs. (Ag/AgCl), PB (pH 7.0)	22.6 - 453	9.05	incubation	[34]
AChE/Cyt c / SiL/ITO	Amperometry	-0.5 V vs. (Ag/AgCl), PB (pH7.0)	10 - 1 x10^6	3.01	incubation	[35]
AChE/Al_2O_3 / SPE	Amperometry	0.25 V vs. (Ag/AgCl), PB (pH 7.0)	100-80 x10^3	10	incubation	[36]
ChOx/PBCB$_{ethaline}$-HNO$_3^{PTD}$	Amperometry	-0.5 V vs. (Ag/AgCl), PB (pH 7.0)	2.5-60	1.6	injection	This work

AChE/CS@TiO_2-CS/rGO/GCE - acetylcholinesterase (AChE) adsorbed on chitosan (CS), TiO_2 sol-gel, and reduced graphene oxide (rGO) based multi-layered immobilization matrix modifying glassy carbon electrode; AChE–Er-GRO–Nafion/GCE - AChE immobilized on electrochemically reduced graphene oxide and Nafion hybrid nanocomposite modified glassy carbon electrode; AChE/Cyt c/SiL/ITO - AChE and cytochrome c (Cyt c) incorporated into mesoporous silica thin films modifying indium tin oxide; AChE/Al_2O_3/SPE - ACHE entrapped in Al_2O_3 screen-printed sol-gel matrix.

Table 3. Recovery test of dichlorvos spiked in orange juice

Sample	Added / nM	Expected / nM	Found / nM	Recovery (%)
1	10	10	10.22 ± 0.04	102.2
2	20	20	19.94 ± 0.02	99.7
3	30	30	31.05 ± 0.04	101.5